2002

Rates of Sedimentation in the Central Arctic Ocean

Jan Backman
Stockholm University

Martin Jakobsson
University of New Hampshire, Durham

Reidar Lovlie
Institute of Solid Earth Physics, Bergen, Norway

Leonid Polyak
Ohio State University - Main Campus

Rates of Sedimentation in the Central Arctic Ocean

Paper Number:
GP71A-0986

[1]Jan Backman, [2]Martin Jakobsson, [3]Reidar Løvlie and [4]Leonid Polyak
[1]Department of Geology and Geochemistry, Stockholm University, Sweden
[2]Center for Coastal and Ocean Mapping/ Joint Hydrographic Center, University of New Hampshire, USA
[3]Institute of Solid Earth Physics, University of Bergen, Norway
[4]Byrd Polar Research Center, Ohio State University, USA

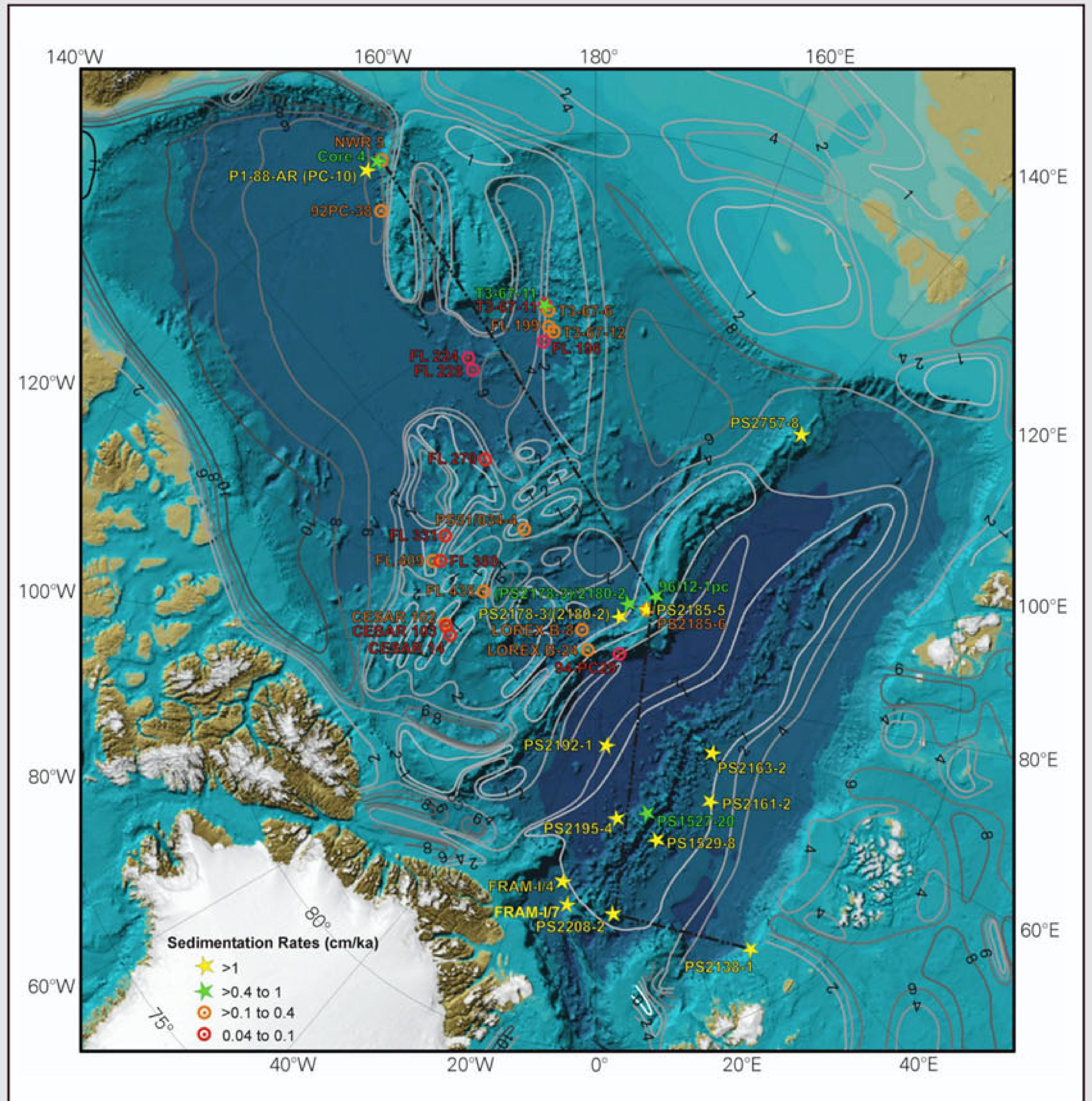

Figure 1. Key cores discussed in this work regarding inferred sedimentation rates (Table 1). The bathymetry is portrayed by the IBCAO bathymetric model (see Jakobsson et al., 2000a). Contour lines represent sediment thickness isopachs in km (from Jackson and Oakey, 1990). Transect of four cores from the Barents slope (PS2138-1), via the Gakkel Ridge (PS1527-20) and the Lomonosov Ridge (96/12-1pc), to the Northwind Ridge (NWR 5), is connected by thick black stippled line. The core correlation along this transect is presented in Figure 3.

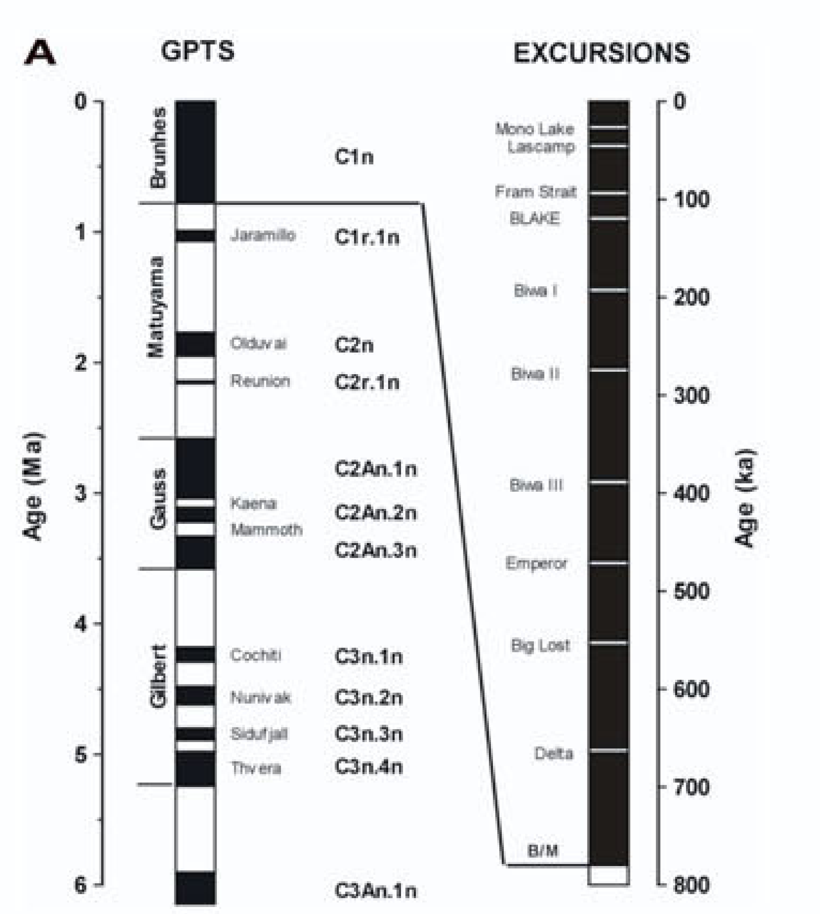

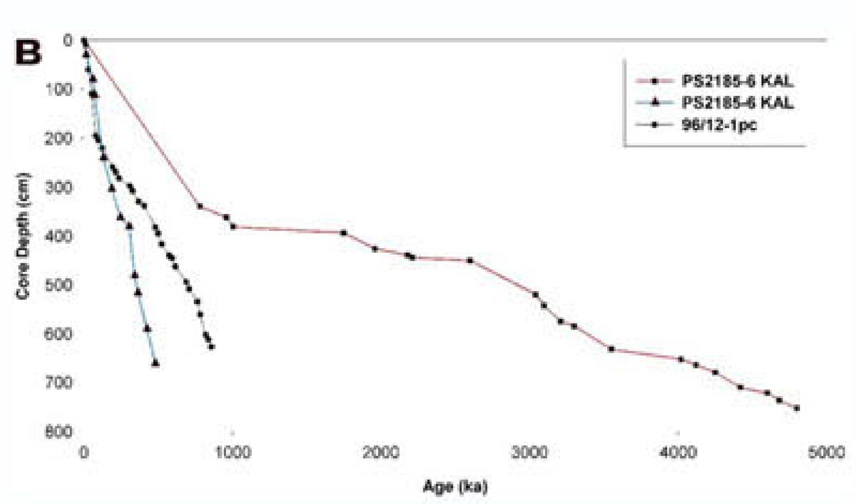

Figure 2. A: Comparison between the Geomagnetic Polarity Time Scale (GPTS) of Cande and Kent (1992) and the Brunhes Chron excursion time scale of Langereis et al. (1997). B: Alternative age-depth relationship for core PS2185-6 from the Lomonosov Ridge (see Figure 1). The excursion scenario (Frederichs, 1995) is plotted with triangles and blue connecting lines and the full polarity reversal scenario (Frederichs, 1995; Spielhagen et al., 1997) with squares and red connecting lines. In addition, the age-depth relationship is plotted for core 96/12-1pc also retrieved from the Lomonosov Ridge (Jakobsson et al., 2000b).

Summary

The Arctic Ocean is presently undergoing geoscientific investigations of the type that occurred during the late 1940's through 1960's in the Atlantic, Indian and Pacific oceans. Seismic reflection and refraction data are scarce in the Arctic Ocean and large areas are virtually unsampled with respect to piston or gravity coring. The vast majority of available cores are less than10 m in length and largely lack biostratigraphically useful calcareous and siliceous microfossils. No drill cores exist from the ridges or deep basins in the central Arctic Ocean. Considering the limited geophysical and geological data available, it is not surprising that current concepts about Arctic Ocean sedimentation rates are diverging. The main point of difference is whether or not strongly subdued rates of sedimentation persisted in the central Arctic Ocean during Plio-Pleistocene times. The low sedimentation rate scenario is based on age models suggesting Plio-Pleistocene rates that vary between about 0.04 and 0.4 cm/ka. This scenario is chiefly derived from cores raised from ridges in the Amerasian Basin and implies that the majority of cores presently available extend well into, or encompass the entire, Pliocene. The contrasting high sedimentation rate scenario is based on age models suggesting rates that vary from about one to a few cm/ka, derived from cores from ridges and basins in both the Amerasian and Eurasian parts of the central Arctic Ocean. The latter scenario implies that most short cores rarely extend beyond the Pleistocene. Early paleomagnetic chronologies of sediment cores retrieved from the Amerasian Basin were based on the assumption that zones with negative inclination represented genuine polarity reversals. The first encountered down-core zone with negative inclination was interpreted to be the Brunhes/Matuyama boundary. This approach yielded mm-scale Plio-Pleistocene sedimentation rates. Biostratigraphy, cyclostratigraphy, and OSL dating, subsequently have indicated that many of these negative inclination changes represent Brunhes geomagnetic excursions, thus providing cm-scale Pleistocene sedimentation rates. Figure 2 show a comparison between the Geomagnetic Polarity Time Scale (GPTS) of Cande and Kent (1992) and the Brunhes Chron excursion time scale of Langereis et al. (1997). All longer-term, Cretaceouos through Cenozoic, sedimentation rates derived from seismic and tectonic models of bedrock age are on the order of cm/ka.

Here we present a review of the two contrasting sedimentation rate scenarios and raise some questions:

- Have two distinctly different modes of deposition governed the Plio-Pleistocene sedimentation in the Arctic, one slow on a mm-scale and the other less so on a cm-scale?
- Are the underlying age models of the two depositional modes realistic?
- If this is the case, can we determine where the two modes apply and why?
- If this is not the case, can we determine which of the two chronological models to reject?

We present a map with published key cores and inferred sedimentation rates (Figure 1) and a sediment core correlation along a transect from the southwestern part of the Amerasian Basin to the southwestern part of the Eurasian Basin (Figure 3) This correlation provides a crucial link between the sediment stratigraphies of the two major Arctic Ocean basins.

References

Cande, S.C., Kent, D.V., 1992. A new geomagnetic polarity time scale for the Late Cretaceous and Cenozoic. Journal of Geophysical Research 97, 13917-13951.

Frederichs, T.,1995. Regional and temporal variations of rock magnetic parameters in Arctic marine sediments. Berichte zur Polarforschung 164,1-212.

Gard, G., 1993. Late Quaternary coccoliths at the North Pole: Evidence of ice-free conditions and rapid sedimentation in the central Arctic Ocean. Geology 21, 227-230.

Jackson, H.R., Oakey, G.N., 1990. Sedimentary thickness map of the Arctic Ocean. In: Grantz et al. (Eds.), The Arctic Ocean Region. Boulder, Geological Society of America, The Geology of North America v. L, Plate 5.

Jakobsson, M., Cherkis, N., Woodward, J., Coakley, B., and Macnab, R., 2000a, A new grid of Arctic bathymetry: A significant resource for scientists and mapmakers, EOS Transactions, American Geophysical Union, v. 81, no. 9, p. 89, 93, 96.

Jakobsson, M., Løvlie, R., Al-Hanbali, H., Arnold, E., Backman, J., Mörth, M., 2000b. Manganese and color cycles in Arctic Ocean sediments constrain Pleistocene chronology. Geology 28, 23-26.

Knies, J., Vogt, C., Stein, R., 1999. Late Quaternary growth and decay of the Svalbard/Barents Sea ice sheet and paleoceanograpic evolution in the adjacent Arctic Ocean. Geo-Marine Letters 18, 195-202.

Langereis, C.G., Dekkers, M J., de Lange, G.J., Paterne, M., van Santvoort, P.J.M., 1997. Magnetostratigraphy and astronomical calibration of the last 1.1 Ma from an eastern Mediterranean piston core and dating of short events in the Brunhes. Geophysical Journal International 129, 75-94.

Matthiessen, J., Knies, J., Nowaczyk, N.R., Stein, R., 2001. Late Quaternary dinoflagellate cyst stratigraphy at the Eurasian continental margin, Arctic Ocean: indications for Atlantic water inflow in the past 150,000 years. Global and Planetary Change 31, 65-86.

Poore, R.Z., Phillips, R.L., Rieck, H.J., 1993. Paloeclimate record for Northwind Ridge, Western Arctic Ocean. Paleoceanography 8, 149-159.

Poore, R. Z., Ishman, S. E., Phillips, L., McNeil, D., 1994. Quaternary stratigraphy and paleoceanography of the Canada Basin, western Arctic Ocean. U.S. Geological Survey Bulletin 2080, pp. 1-32.

Spielhagen, R.F., Bonani, G., Eisenhauer, A., Frank, M., Frederichs, T., Kassens, H., Kubik, P.W., Mangini, A., Nørgaard-Pedersen, N., Nowaczyk, N.R., Schäper, S., Stein, R., Thiede, J., Tiedemann, R., Wahsner, M., 1997. Arctic Ocean evidence for late Quaternary initiation of northern Eurasian ice sheets. Geology 25, 783-786.

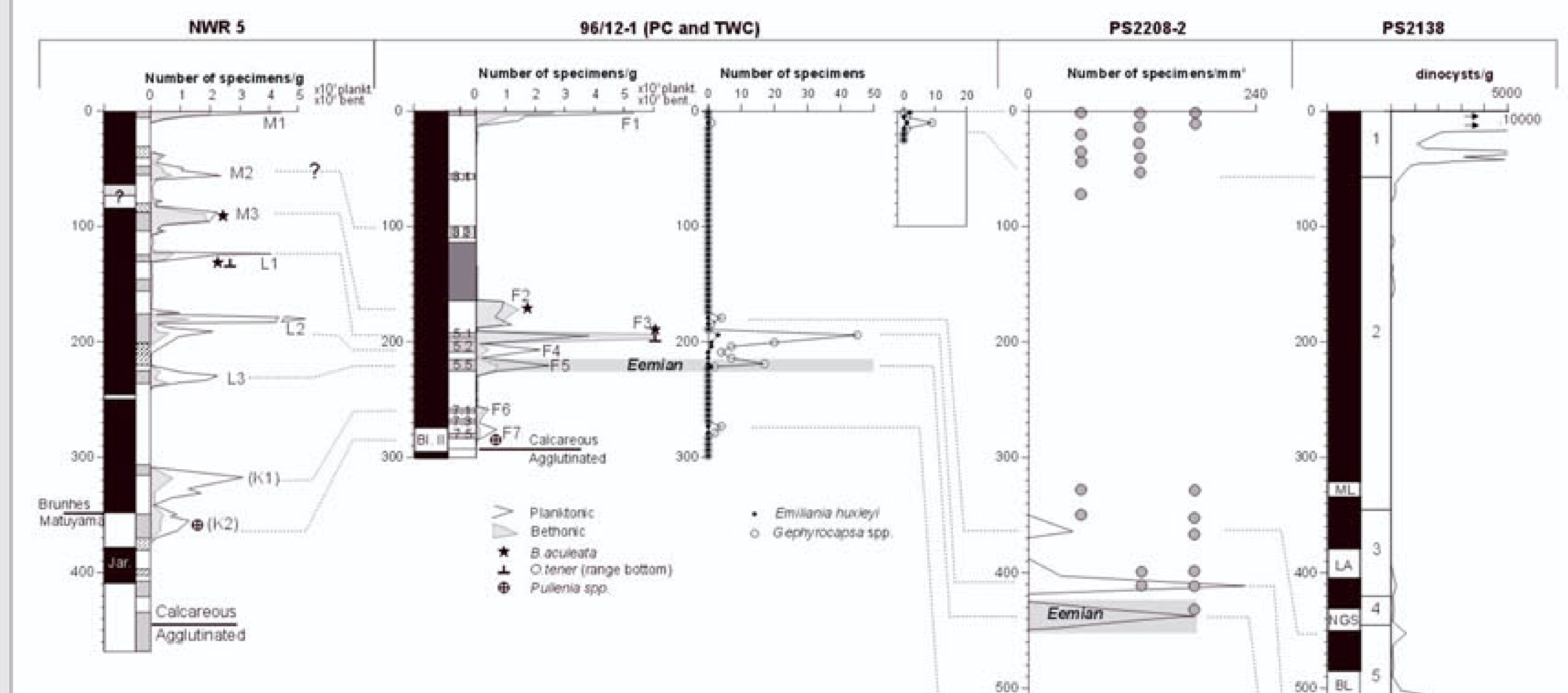

Figure 3. Correlation along the transect shown in Figure 1. The correlation is mainly based on foraminiferal stratigraphies between cores 96/12-1pc and NWR 5 (= PI88-P5) (Poore et al., 1993; 1994). The continuation into the Eurasian Basin is based on biostratigraphy by linking fluctuations of nannofossil abundance peaks during MIS 5.5, 5.3 and 5.1 in core 96/12-1pc with concentration fluctuations of dinoflagellate taxa in core PS2138-1 (Knies et al., 1999; Mathiessen et al., 2001) from the Barents Sea margin. Matthiessen and colleagues suggest that dinoflagellate cyst events are caused by variable inflow of relatively warm Atlantic water into the Arctic Ocean during periods of warm climate conditions. By using such biostratigraphic signals caused by climatic variability in the glacial/interglacial system, it is possible to also include core 2208-2 (Gard, 1993) from the Gakkel Ridge into the correlation transect.

Table 1. Sedimentation rates (cm/ka) in cores from the central Arctic Ocean. In the four cases where two cores occur in one row, core designations in bold face refer to the core that shows the water depth. A few cores are listed twice, when published estimates of sedimentation rates differ widely. Most sedimentation rate values (cm/ka) are approximative because core depths of age control points are predominantly estimated from published figures.

CORE	AUTHOR	DEPTH	cm_ka	Age Control Notes Referring to Published Results
94-PC29	Grantz et al. 2001 (fig. 7)	3010	0.04	Top core to 220 cm ('lower Pliocene') if age is 5.0 Ma; 0.06 cm/ka if age is 4.0 Ma
FL 224	Clark et al. 1980 (fig. 29)	3467	0.05	Top Gauss to top 'polarity epoch 5' (=top Chron C3An.1n)
FL 270	Clark et al. 1980 (fig. 30)	3280	0.06	Top core to Brunhes/Matuyama boundary
FL 196	Clark et al. 1984 (fig. 4)	3327	0.06	Top core to Brunhes/Matuyama boundary
T3-67-11	Herman 1974 (fig. 20)	2810	0.06	Top core to middle part of Mammoth Subchron
CESAR 14	Aksu and Mudie 1985 (fig. 2)	1370	0.08	Top core to Gauss/Gilbert boundary
FL 331	Clark et al. 1980 (fig. 30)	2659	0.09	Top core to Brunhes/Matuyama boundary
FL 380	Clark et al. 2000 (fig. 2)	2401	0.09	Top core to unit A assuming linear depth scale in fig. 2 and that base unit A2 is 345-60 cm = 285 cm
CESAR 103	Aksu and Mudie 1985 (fig. 2)	1585	0.10	Top core to Brunhes/Matuyama boundary
FL 224	Steuerwald et al. 1968 (fig. 1)	3467	0.10	Base Brunhes to top Gauss (base Brunhes of Steuerwald fig. 1 = top Gauss of Clark et al. 1980 fig. 29)
FL 228	Clark et al. 1980 (fig. 30)	3632	0.10	Top core to Brunhes/Matuyama boundary
FL 435	Clark et al. 1980 (fig. 30)	2272	0.14	Top core to Brunhes/Matuyama boundary
LOREX B-24	Morris et al. 1985 (figs. 3 9)	0	0.16	Top core to base unit M inferred at 400 ka (=427 ka if B/M boundary = 780 ka)
T3-67-12	Witte and Kent 1987 (table 1)	2867	0.16	Top core to base Olduvai
PS51/034-4	Jokat et al. 1999a (fig. 3)	2071	0.17	Lithostratigraphic unit B/C boundary at 1.9 Ma
PS2185-6	Spielhagen et al. 1997 (fig. 2)	1052	0.18	Top core to Gauss/Gilbert boundary
LOREX B-8	Morris et al. 1985 (figs. 2 9)	0	0.18	Top core to unit K inferred to hold Brunhes/Matuyama boundary
FL 409	Clark et al. 1980 (fig. 30)	2742	0.19	Top core to Brunhes/Matuyama boundary
92PC-38	Phillips and Grantz 2001 (fig. 10)	1917	0.20	Top core to 'initiation of glacial ice-rafting at 2.7 Ma'
T3-67-6	Witte and Kent 1987 (table 1)	2815	0.25	Top core to base Jaramillo
FL 199	Clark et al. 1984 (fig. 2)	2988	0.26	Top core to Brunhes/Matuyama boundary
NWR 5	Poore et al. 1993 (fig. 2)	0	0.38	Top core to base Jaramillo
PS2178-3/**2180-2**	Nowaczyk et al. 2001; age model 2	3991	0.54	Paleointensity correlation; composite depth: 1000 - 1150 cm
96/12-1pc	Jakobsson et al. 2000 (fig. 3)	1003	0.72	Top core to Brunhes/Matuyama boundary
Core 4	Phillips and Grantz 1997 (fig. 8)	2430	0.86	Top core to Brunhes/Matuyama boundary; 'composite stratigraphic section of cores 4 5 and 9'
T3-67-11	Sejrup et al. 1984	2810	0.87	Minimum rate ('260 cm depth...younger than 300 kyr'; amino acid epimerimisation and biostratigraphy
PS1527-20	Baumann 1990 (fig. 2c)	3780	1.0	Coccolith abundance peak in MIS 5 with E. huxleyi
PS2178-3/**2180-2**	Nowaczyk et al. 2001; age model 2	3991	1.0	Paleointensity correlation; omposite depth: 200 - 1000 cm
PS2185-5	Gard 1993 (table 1)	1051	1.4	Holocene coccolith data (represents the average Holocene rate on the Lomonosov Ridge)
PS2757-8	Mathiessen et al. 2001 (fig. 9)	1230	1.6	Dinoflagellate cyst stratigraphy correlated to MIS 5/6 boundary
PS2195-4	Gard 1993 (table 1)	3873	1.7	Holocene coccolith data (represents the average Holocene rate in the Amundsen Basin)
FRAM-I/4	Markussen et al. 1985 (fig. 4)	3820	2.0	Oxygen isotopes through Termination 1A
FRAM-I/7	Markussen et al. 1985 (fig. 4)	2990	2.0	Oxygen isotopes through Termination 1A; 3.5 cm during MIS 2
PS2163-2	Gard 1993 (table 1)	3047	2.9	Holocene coccolith data (represents the average Holocene rate on the Gakkel Ridge)
PS1529-8	Baumann 1990 (fig. 2c)	2917	3.0	Coccolith abundance peak in MIS 5 with E. huxleyi
PS2208-2	Aldahan et al. 2000 (fig. 7)	3682	3.0	10-Be dating through MIS 9
PS2178-3/2180-2	Nowaczyk et al. 2001; age model 1	4009	3.8	Paleointensity correlation; composite depth: 200 - 1250 cm
PS2178-3/2180-2	Nowaczyk et al. 2001; age model 1+2	4009	4.0	Paleointensity correlation; composite depth: 0 - 200 cm
PS2208-2	Gard 1993 (fig. 5)	3682	4.0	Coccolith abundance peak in MIS 5 with E. huxleyi
PS2161-2	Gard 1993 (table 1)	4005	5.0	Holocene coccolith data (represents the average Holocene rate in the Nansen Basin)
P1-88-AR (PC-10)	Grantz et al. 1996 (fig. 8)	3899	120.0	Top core to 847 cm; linear regression of seven radiocarbon ages (r=0.9913)
PS2138-1	Mathiessen et al. 2001 (fig. 3)	995	5	Linear sedimentation rate from first used C14 date at 65 cm (12,999 BP). C14 dates further down core show larger sedimentation rates through MIS 2
CESAR 102	Macko and Aksu 1986 (fig. 2)	1495	0.11	Top core to Brunhes/Matuyama boundary
PS2192-1	Gard 1993 (table 1)	4375	2.1	Holocene coccolith data

*The references in this table are not, due to the large amount, further listed in the reference list on this poster